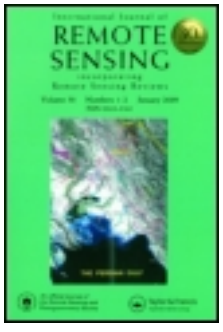


International Journal of Remote Sensing

Publication details, including instructions for authors and subscription information:
http://www.tandfonline.com/loi/tres20

# Northward drift of suspended sediments in the Yangtze estuary in spring

Xinfeng Zhang[abc], Fuxiang Hu[d], Jian Zhang[abc] & Danling Tang[e]

[a] College of Marine Sciences, Shanghai Ocean University, Shanghai 201306, China

[b] The Key Laboratory of Sustainable Exploitation of Oceanic Fisheries Resources, Ministry of Education, Shanghai Ocean University, Shanghai 201306, China

[c] National Engineering Research Centre for Oceanic Fisheries, Shanghai Ocean University, Shanghai 201306, China

[d] Tokyo University of Marine Science and Technology, Minato-Ku, Tokyo 108-8477, Japan

[e] Centre of Remote Sensing on Marine Ecology/Environment, State Key Laboratory of Tropical Oceanography, South China Sea Institute of Oceanology, Chinese Academy of Sciences, Guangzhou 510301, China

Published online: 02 Jun 2014.

To cite this article: Xinfeng Zhang, Fuxiang Hu, Jian Zhang & Danling Tang (2014): Northward drift of suspended sediments in the Yangtze estuary in spring, International Journal of Remote Sensing, DOI: 10.1080/01431161.2014.916455

To link to this article: http://dx.doi.org/10.1080/01431161.2014.916455

*International Journal of Remote Sensing*, 2014
http://dx.doi.org/10.1080/01431161.2014.916455

Taylor & Francis
Taylor & Francis Group

# Northward drift of suspended sediments in the Yangtze estuary in spring

Xinfeng Zhang[a,b,c], Fuxiang Hu[d], Jian Zhang[a,b,c], and Danling Tang[e]*

[a]*College of Marine Sciences, Shanghai Ocean University, Shanghai 201306, China;* [b]*The Key Laboratory of Sustainable Exploitation of Oceanic Fisheries Resources, Ministry of Education, Shanghai Ocean University, Shanghai 201306, China;* [c]*National Engineering Research Centre for Oceanic Fisheries, Shanghai Ocean University, Shanghai 201306, China;* [d]*Tokyo University of Marine Science and Technology, Minato-Ku, Tokyo 108-8477, Japan;* [e]*Centre of Remote Sensing on Marine Ecology/Environment, State Key Laboratory of Tropical Oceanography, South China Sea Institute of Oceanology, Chinese Academy of Sciences, Guangzhou 510301, China*

(*Received 19 October 2013; accepted 13 December 2013*)

The spatial distribution of suspended sediment concentration (SSC) in spring (February–April) from 2007 to 2013 in the Yangtze (Changjiang) estuary and coastal seas was analysed using remote-sensing data. The results indicated that areas of high SSC drifted northwards along the coast about 100 km away from the Yangtze estuary. SSC increased considerably in both mass and area in 2013. The first principal component analysis (PCA) pattern explained the dominant spatial distribution pattern of SSC in the study area. This highly clustered controlling pattern may have been caused by the joint effects of Yangtze diluted water (YDW), the Taiwan Warm Current (TWC), coastal currents, northeasterly winds, and the shallow coastal shelf. The SSC dispersed and extended into a wide area, and the main range of sediment concentration was located in an area the shape of a trapezium (31.9° N–33.8° N, 122° E–125.5° E, 30.7° N–32.6° N). YDW and the TWC could be the main reason for this northward drift of SSC. The long-term sinking of suspended sediment in clustered areas may have contributed considerably to the formation of the shallow coastal shelf above the 60 m isobath.



## 1. Introduction

The Yangtze (Changjiang) River is the largest river in Asia. The Yangtze estuary is located on the east coast of China and includes some of the coastal waters of the East China Sea (ECS) (Figure 1). Discharges from the river cause severe pollution to the estuarine and coastal ecosystem and the environment of the ECS, and also to the Pacific Ocean. Suspended sediment concentration (SSC) plays an important role in this type of pollution. The Yangtze estuary and coastal waters are characterized by suspended sediments at a wide range of concentrations (Zhang et al. 2007; Shen et al. 2010). The transport and subsequent dispersal of SSC, from the coastal land to the ocean, directly affects the marine environment and biological productivity (such as phytoplankton and fisheries) of the oceans (Witt and Siegel 2000; Yan and Tang 2009; Zhang et al. 2009). However, it is usually difficult to investigate the distribution and transportation of SSC and to track its pathway using traditional approaches and techniques. The spatial distribution of SSC in estuarine and coastal waters is quite complicated and is strongly affected by

*Corresponding author. Email: lingzistdl@126.com

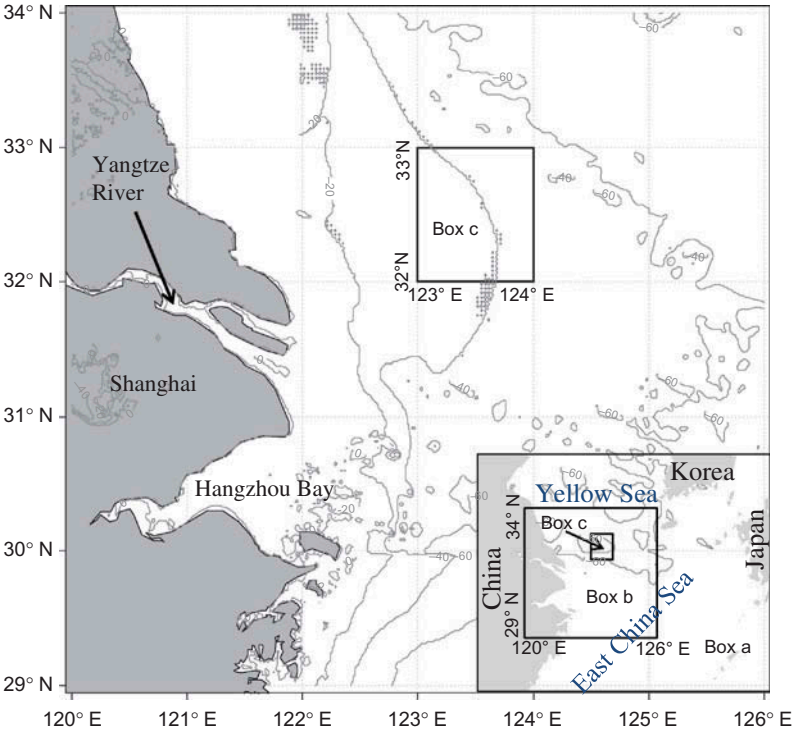


Figure 1. Location of study area (box b) and sampling area 1° × 1° (box c: 32° N–33° N, 123° E–124° E) between the Yellow Sea and the East China Sea.

variation in seasonal riverine discharges, waves, currents, and wind-driven resuspension of bottom sediments (Chen et al. 2003, Krivtsov, Howarth, and Jones 2009).

The dispersal of the Yangtze influx into the ECS forms turbid plumes extending eastwards over an area of 104–105 $km^2$ (Tang et al. 1998; Zhang et al. 2007). Based on collected data, Guo et al. (2002) studied the distribution of suspended matter in the northern ECS in winter and summer, and found that the factors most influential in the distribution and transport of suspended matter were current circulation, storms, and tidal currents, and the controlling factor was current circulation. Based on field observations of SSC, Pang et al. (2003) concluded that suspended matter from the Yangtze River was always transported in a southeasterly direction, regardless of season. About 87% of the annual total sediment discharges in the flood season (i.e. June–September). About 50% of the sediments carried by the Yangtze River are accumulated at the river mouth, forming large submerged deltas and mouth bars (Shen and Pan 2001). Chen et al. (2003) found that high levels of SSC in the Yangtze estuary were related to the presence of algal blooms in summer. Many other studies have also researched the chemical composition, transportation, formation, and variation of SSC in the Yangtze estuary by *in situ* measurements (Li, Shi, and Shen 1994, 2001; Wu, Shen, and Xiao 2001; Gao et al. 2005).

Remote-sensing approaches have been widely used to track and investigate the distribution of SSC, rainfall, sea-surface temperature, phytoplankton, etc. in estuaries and on the ocean surface (Shen et al. 2010; Yan and Tang 2009; Zhang et al. 2009). Using satellite data, Wang and Jiang (2008) studied the seasonal variation in SSC at a

larger scale (including the Yellow Sea and ECS). Although the above studies have advanced our understanding of the dynamics of SSC distribution in the Yangtze estuary and coastal waters, few have focused on the SSC distribution pattern in spring using remote-sensing data. Spring (February–April) is a relatively dry season for runoff from the Yangtze River, when it may be more likely that the SSC will cluster and produce an entirely different spatial pattern. In this article, we aimed to study the spatial pattern of SSC in spring in the Yangtze estuary and adjacent coastal seas using 7 years of MODIS satellite remote-sensing data, from 2007 to 2013, and to investigate the effects of wind and current circulation on the SSC.



## 2. Study area and satellite data

The study area is located between 29° N and 34° N, 120° E and 126° E in the Yangtze estuary and adjacent coastal seas (Figure 1), covering the Yangtze estuary, Hangzhou Bay, coastal waters, and also some adjoining deep-sea areas of the ECS. In order to avoid the influence of very turbid coastal waters, one sampling area of 1° × 1° (32° N–33° N, 123° E–124° E, marked as Box c in Figure 1) was selected as the main concentrated surface area of suspended sediment.

Satellite remote-sensing reflectance (RSR) is monotonically related to the physical parameters of SSC. This relationship means that retrieving physical properties from a spectrum is feasible (Cheng and Zhang 2010). Shen et al. (2010) found that the sensitivity and saturation level of RSR to SSC are dependent on wavelengths and SSC levels, and Shen et al. (2010) also retrieved SSC data from RSR in the Yangtze estuary and coastal waters using a semi-empirical transfer model. Based on the above studies, it is reasonable to use the RSR of seawater as a measure for SSC. In the present study, the satellite MODIS RSR values at 555 nm ($sr^{-1}$) are used as a surrogate for SSC and we refer to RSR as SSC hereafter.

The monthly RSR (SSC) data of 4 km resolution at 555 nm ($sr^{-1}$) were obtained from the Ocean Color Time Series Project (National Aeronautics and Space Administration, USA) (http://reason.gsfc.nasa.gov/Giovanni/). Three months in spring (February–April) over the 7 years from 2007 to 2013 were chosen. The wind vector satellite data at 0.25° resolution in spring 2009 were obtained from PODAAC-ESIP (http://poet.jpl.nasa.gov). PODAAC-ESIP can only offer wind data before 2010, so we used those for 2009 as representative to investigate the correlation between wind and SSC in the study area, because the wind field in the study area in spring is similar every year.

## 3. Methods

Principal component analysis (PCA) was initially applied to a time series of meteorological data (Lorenz 1956). The PCA method has also been used to identify dominant spatial and temporal patterns from a series of remote-sensing data (Tew-Kai and Marsac 2009; Nezlin and Mcwilliams 2003). SSC data in the 5 years from 2007 to 2011 were used to undertake a PCA analysis, and those for 2012 and 2013 were used to verify the main PCA pattern. The PCA process was as follows.

To set up a spatial data matrix of SSC:

$$\mathbf{X} = [\mathrm{SSC2007}, \mathrm{SSC2008}, \mathrm{SSC2009}, \mathrm{SSC2010}, \mathrm{SSC2011}]. \quad (1)$$

To compute the covariance matrix:

$$\mathbf{C} = (1/n)\mathbf{X}\mathbf{X}^{\mathrm{T}}, \tag{2}$$

where $n$ is the number of data in the columns of $\mathbf{X}$. To solve the eigenvalues and eigenvectors of $\mathbf{C}$; PCA patterns can be estimated by $\mathbf{C}$:

$$\mathbf{CE} = \mathbf{AE}. \tag{3}$$

The eigenvector matrix $\mathbf{E}$ contains the PCA patterns, and matrix $\mathbf{A}$ contains the eigenvalues on its diagonal.

To calculate the principal component (PC); PCA can be projected on the original data matrix $\mathbf{X}$:

$$\mathrm{PC} = \mathbf{E}^{\mathrm{T}}\mathrm{X}. \tag{4}$$

Then the first column of PC is simply the coefficients of the first PCA pattern.

The first few PCAs explain the majority of the variance of data. When used as a linear predictor, the first PCA explains the greatest fraction of total variance.

The correlation between SSC and wind was analysed using the Pearson correlation coefficient $r$. The data of SSC and wind were standardized before the statistical test. The test for the Pearson correlation coefficient $r$ was conducted by an ordinary $t$-test. In order to compare SSC and wind at the same scale, we aggregated the SSC data from 4 km to 0.25° resolution.

## 4. Results

### 4.1. *Controlling spatial pattern of SSC in spring*

The spatial patterns of SSC distribution in spring from 2007 to 2011 were very similar (Figure 2). SSC dispersed and extended over a wide range from 122° E to 126° E (about 400 km), and from 30° N to 34° N (about 440 km). SSC was higher inshore and lower offshore. However, there was an abnormal phenomenon whereby areas of high SSC did not directly surround the Yangtze estuary but drifted significantly northwards along the coast by about 100 km. In a larger-scale investigation of pigment concentrations, Tang et al. (2004) also found a similar area of high SSC near the Yangtze estuary. Data in some very turbid coastal waters cannot be validly retrieved by MODIS due using the available algorithms (IOCCG 2000), and hence the missing (invalid) values of SSC nearest the coast were not included in the remote-sensing images.

To further investigate the dominant spatial pattern of the distribution of SSC in spring, five spatial patterns were obtained from PCA analysis, which indicated that the proportion of variance of the first PCA pattern was considerably higher (86.33%) than the sum of others. Owing to the very small proportion of the other four PCA patterns (each <5%), only the first distribution pattern of SSC is given here (Figure 3). It was clear that the range and dispersal trend of SSC in the latter 2 years (2012 and 2013) was very close and similar to the first PCA pattern (Figure 4). This verified again that the first PCA pattern was the dominant pattern of SSC distribution in the study area. The first PCA pattern demonstrated clearly the abnormal phenomenon of the distribution of SSC, which was that the area of high SSC did not surround the Yangtze estuary directly but drifted significantly northwards about 100 km along the coast.

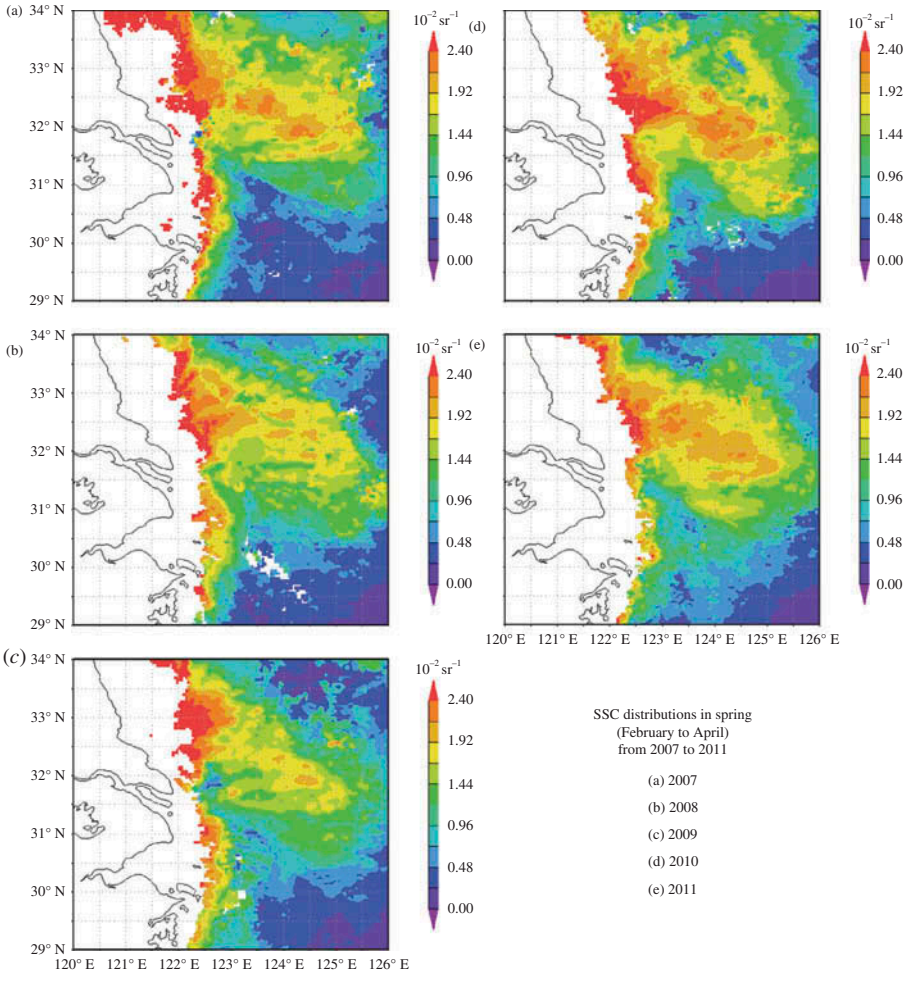


Figure 2. Spatial distributions of SSC in spring (February–April) from 2007 to 2011.

### 4.2. *Variation of SSC in spring from 2007 to 2013*

In the sampling area, the variation in SSC was marginal from 2007 to 2009, but notably increased after 2009 and reached a peak in 2013 (Figure 5). There was also a general trend of increasing SSC from 2007 to 2013; SSC in 2010 and 2013 was obviously higher than in the other years, and this also coincided with the widest dispersal range in 2010 and 2013. This finding suggests that the suspended sediment and associate contaminants discharged from the Yangtze River notably increased in 2013.

### 4.3. *Effects of wind on SSC*

The wind field is demonstrably controlled by a northeasterly wind in spring (Figure 6). Because of the direction of this wind, the two components (zonal and meridional) of remote-sensing wind vector data were mostly below zero (i.e. negative). To avoid the influence of the negative wind vector direction in two-dimensional coordinates, the

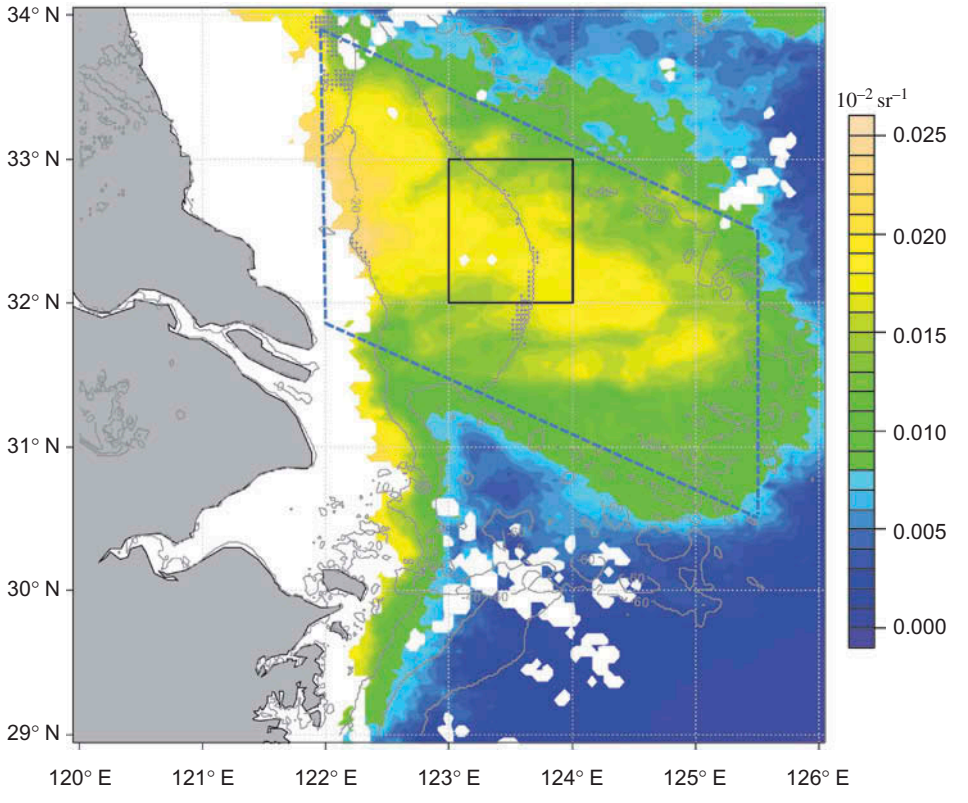


Figure 3. SSC distributions in the first PCA pattern in spring (February–April) for the years 2007–2011. The dashed trapezium indicates the main range of SSC (31.9° N–33.8° N, 122° E–125.5° E, 30.7° N–32.6° N).

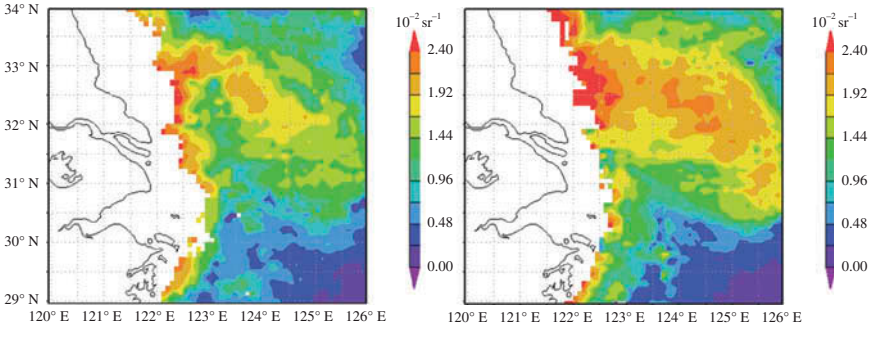


Figure 4. Spatial distribution of SSC in spring (February–April) for 2012 and 2013.

opposite values (mainly positive) of the two components were used in the statistical testing of the correlation between the components of wind and SSC. An interesting phenomenon found was that the zonal component (along longitude) of the wind vector affected SSC weakly either positively or negatively ($|r| < 0.3$), but the meridional component (along latitude) of wind showed a significant negative relation with SSC

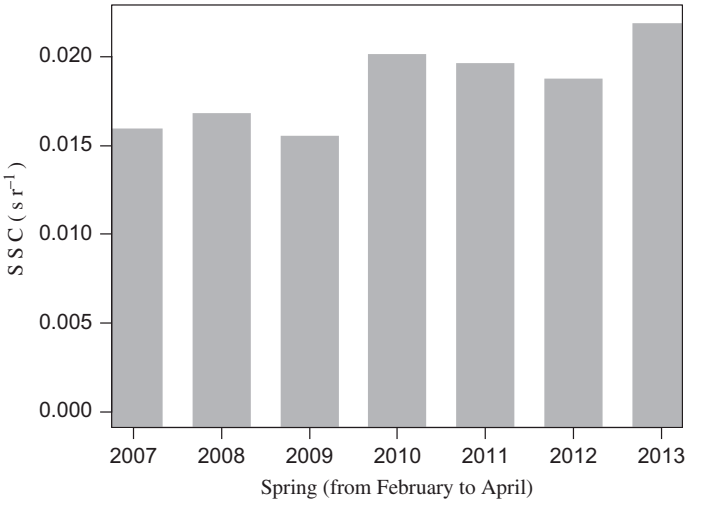


Figure 5. Variation in SSC in spring (February–April) from 2007 to 2013 in the sampling area (Box c in Figure 1: 32° N–33° N, 123° E–124° E).

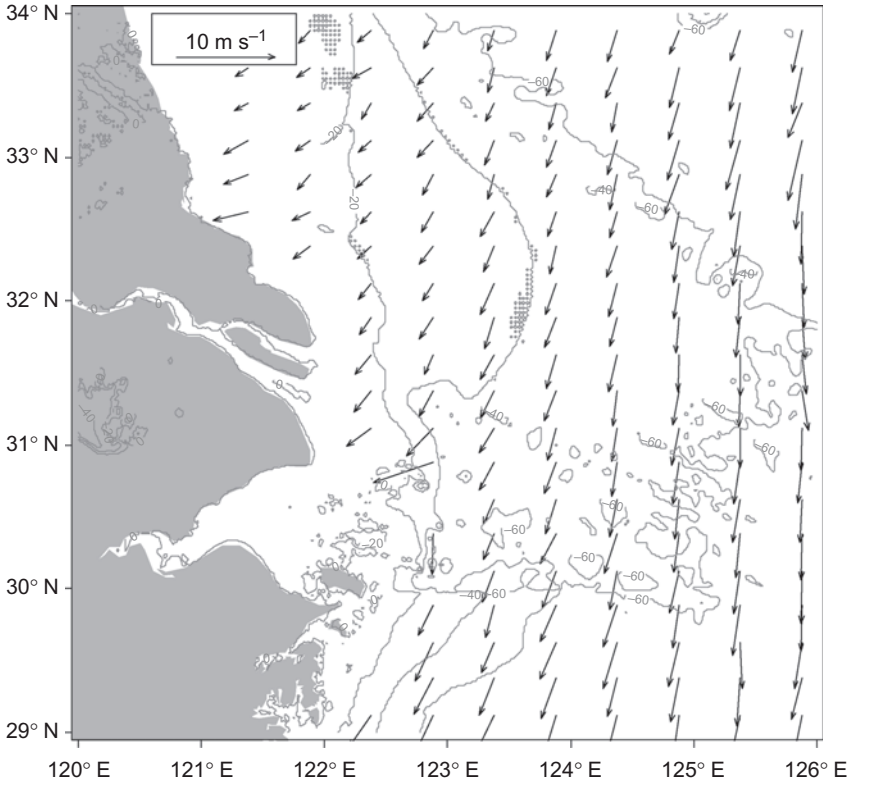


Figure 6. Wind field in spring (February–April) 2009.

Table 1. Correlation test between SSC and wind vector.

| Time | Along longitude | Along latitude | SSC and wind speed |
|---|---|---|---|
| February | −0.233 | −0.265 | −0.26 |
| March | −0.008* | −0.624 | −0.624 |
| April | 0.296 | −0.61 | −0.184 |
| Spring | 0.248 | −0.72 | −0.637 |

Note: All $p$-values <0.01, except * ($p$-value = 0.89).

($r$ = –0.72) (Table 1). However, wind magnitude (speed with no direction) influenced SSC negatively and significantly ($r$ = –0.637).

## 5. Discussion

### 5.1. *Trends in SSC variation*

The spatial distribution of SSC dispersed and extended over a wide range, from 122° E to 126° E (about 400 km), and from 30° N to 34° N (about 440 km). This range considerably exceeded that found by Zhang et al. (2007), being widest in 2010 and 2013 (Figures 2 and 4). Wang and Jiang (2008) found that the transportation of suspended sediment barely reached 124° E in summer or 126° E in winter prior to 2007, which was due to obstruction by the Taiwan Warm Current (TWC) and the Kuroshio current in the southern Yellow Sea and ECS (Pang et al. 2003; Wang and Jiang 2008). Our results indicate that the transportation of suspended sediment could reach, and slightly exceed, 126° E in spring, after 2009 (Figures 2 and 4). This phenomenon was more obvious in 2013 (Figure 4). SSC increased considerably both in mass and area in 2013 (Figures 4 and 5). The main range of SSC is located in an area shaped like a trapezium (31.9° N–33.8° N, 122° E–125.5° E, 30.7° N–32.6° N) (Figure 3).

### 5.2. *Influence of northeasterly wind and shallow coastal shelf on SSC*

It is understood that SSC is usually positively affected by wind-induced resuspension in ordinary ocean waters (Powell, Cloern, and Huzzey 1989; Schoellhamer 1996; Warner et al. 2004). The effects of wind on suspended particulate matter depended on the wind speed in the Mandovi Estuary, where SSC had a positive correlation with strong winds (>5.0 m $s^{-1}$) but a negative correlation with weak winds (Kessarkar et al. 2009). In the present study, the wind speed was usually less than 4.2 m $s^{-1}$, and the meridional component (along latitude, southwards) of the wind vector had a significant negative relationship with SSC ($r$ = –0.72) (Table 1). This indicates that the southward component of the wind vector could partially reduce SSC and obstruct the northward drift of the area of high SSC.

About half of the area of high SSC was located in the shallow waters above the isobath of 40 m, and almost the entire area of high SSC was located above the isobath of 60 m (Figures 1 and 3), and a small part of this area was above the 20 m isobath. Shallow waters are not conducive to the sinking of suspended sediments, and wind and waves can resuspend some sediment from the bottom to the surface of the water. The shallow coastal shelf might represent an obstruction for the northward drift of SSC, and hence partly contribute to the clustering of high SSC.

The eastwards extension of the isobaths of 40 and 60 m coincided well with the area of high SSC (Figure 3). It was clear that the highly clustered controlling pattern of SSC,

and its sinking in the long term, contributed much to the formation of the shallow coastal shelf above the 60 m isobath.

### 5.3. *Impacts of Yangtze diluted water and currents on the northward drift of SSC*

Based on field observations of SSC in July and August 2001 and January 2002, Pang et al. (2003) concluded that suspended matter, discharged from the Yangtze River, was always transported in a southeasterly direction, regardless of season. However, by using remote-sensing methods, the results of the present study showed clearly that the SSC headed northeastwards first and then turned southeastwards (Figures 2 and 3).

Three main currents exist in the study area (Figures 7 and 8): the coastal current that flows southwards; the stronger current of the TWC that flows towards the Yangtze estuary from the southeast and changes little between the seasons (Guo et al. 2002; Su 1989); and the Yangtze diluted water (YDW) current. The YDW usually splits into two branches upon entering the shelf: the surface layer of clearer water, first flowing northeastwards and then rotating clockwise east of 122.5° E; and the deeper turbid diluted water flowing southeastwards along the coast (Figure 8) (Chen et al. 2003, Ichikawa and Beardsley 2002).

Using *in situ* investigations, some studies also found areas of high SSC in the coastal waters to the north of the Yangtze estuary from 32° to 33° N. The main reason for this was considered to be the coastal currents and winds that drove the north coastal suspended sediments along the coast to the south (Guo et al. 1999; Xing et al. 2010; Guo et al. 2002). The mean annual sediment input from the Yangtze river reaches $0.48 \times 10^9$ tonnes per year and is the major source of suspended sediments in the Yangtze estuary and the ECS (Milliman and Meade 1983; Shen and Pan 2001; Liu et al. 2007). The northeastern branch of the YDW carries masses of suspended sediment into the ECS (Chen et al. 2003). The central transportation path for areas of high SSC is similar to the northeastwards path of

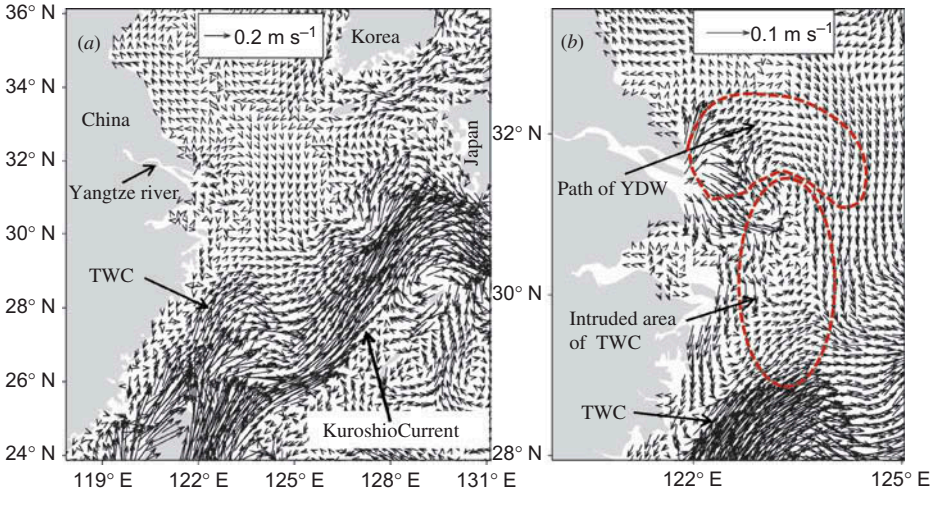


Figure 7. Surface current circulation (mean pattern) in spring (February–April) 2012. The current data are taken from the Navy Coastal Ocean Model (NCOM) of NOAA (http://ecowatch.ncddc.noaa.gov/). (*a*) Surface current in the larger area; (*b*) surface current in the central region near the Yangtze estuary.

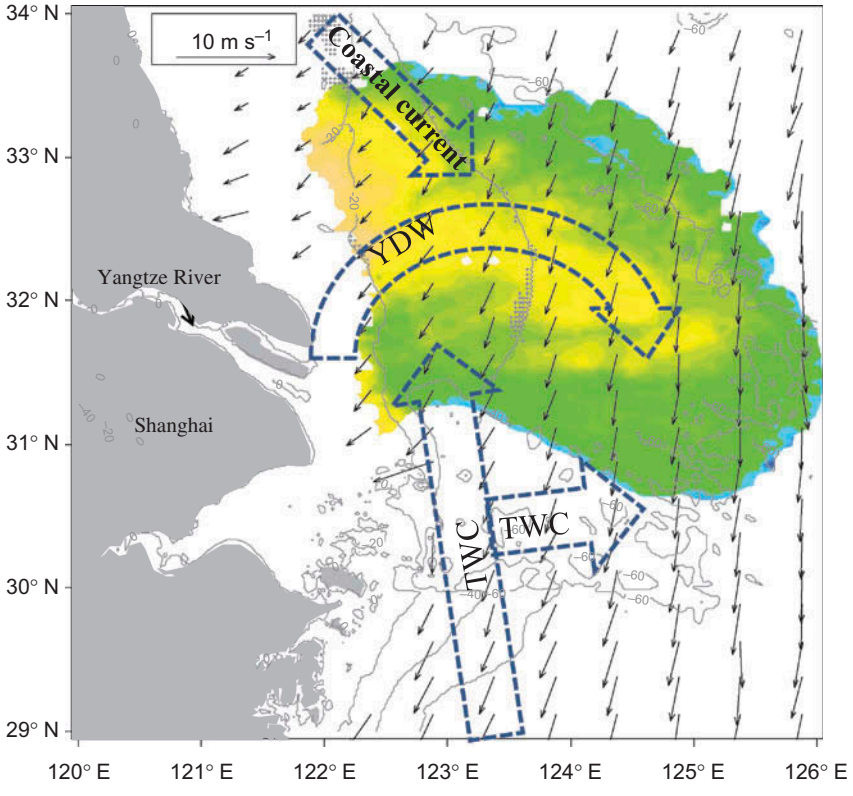


Figure 8. Suspended sediment drift related to wind and current circulation in the Yangtze estuary and coastal seas. The current circulation is from Figure 7 and is also referred to Chen et al. (2003).

the YDW (Figures 3, 7(*b*) and 8). Comparison of these two paths is associated with the main supply to SSC in the Yangtze estuary and ECS, and it is reasonable to assume that the majority of suspended sediments in the high concentration area (31–33° N, 122–125° E) are mainly from the Yangtze river inputs, and this northwards drift of the area of high SSC is mainly caused by the YDW. An area of very low SSC appeared in the intruded area of the TWC from 29° to 31° N and 123° to 124° E (Figures 3, 7(*b*) and 8). It is evident that the intrusions of the TWC contributed greatly to this northwards drift of SSC and enhanced its clustering. The further dispersal of areas of high SSC did not occur directly eastwards but turned southeastwards, east of 123° E. The driving of the southwards coastal current may play a critical role. The eastwards transportation of SSC barely crossed 126.5° E, the main reason probably being obstruction by the Kuroshio Current (Figure 7(*a*)).

Riverine discharges, winds, and currents are important influential factors in SSC distribution in the Yangtze estuary and ECS (Chen et al. 2003, Krivtsov, Howarth, and Jones 2009, Wang and Jiang 2008). In the present study, the combination of the southward coastal current, northeasterly winds, and northwards TWC may have enhanced the clustering of high SSC. It shows clearly that the northwards drift of SSC and the currents are closely related (Figures 3 and 7(*b*)). It is evident that the joint effects of YDW, TWC,

coastal current, northeasterly winds, and a shallow coastal continental shelf cause the clustered spatial pattern of SSC distribution in spring (Figure 8).

## 6. Conclusions

In spring, areas of high SSC drifted significantly northwards along the coast for about 100 km, but did not directly surround the Yangtze estuary. The transportation of suspended sediment reaches, and slightly exceeds, 126° E in spring. SSC increased markedly in both mass and area in 2013.

The YDW and TWC could be the main reason for the northwards drift of SSC. The first PCA pattern explained the dominant spatial pattern of SSC distribution in the study area. This highly clustered spatial pattern of SSC may have been caused by the joint influences of YDW, TWC, coastal current, northeasterly winds, and shallow coastal shelf. The clustered SSC, and its sinking in the long term, contributed much to the formation of the shallow coastal shelf above the 60 m isobath.

## Acknowledgement

We wish to thank Prof. Song Hu for his help with data analysis.

## Funding

This work was supported by the following research grants: Specialized research fund for the doctoral programme of higher education [no. 20103104120006]; Doctoral Fund of Shanghai Ocean University [no. A-2400-10-0137]; the Group Project Program of State Key Laboratory of Tropical Oceanography, South China Sea Institute of Oceanology, Chinese Academy of Sciences [LTOZZ-1201]; and the National Natural Sciences Fund [no. NSFC31001138].

## References

Chen, C., J. Zhu, R. C. Beardsley, and P. J. S. Franks. 2003. "Physical-Biological Sources for Dense Algal Blooms near the Changjiang River." *Geophysical Research Letters* 30 (10): 1515. doi:10.1029/2002GL016391.

Cheng, L., and Y. Zhang. 2010. "Numerical Simulation in Remote-Sensing Reflectance of Suspended Sediment Water." *Information Science and Engineering (ICISE), 2nd International Conference*, Hangzhou, December 4–6, 6733–6736.

Gao, J., Y. Wang, S. Pan, A. Wang, and Y. Yang. 2005. "Formation Mechanisms of Turbidity Maximum in Changjiang Estuary during the Dry Season." [In Chinese.] *Journal of Sediment Research* 5: 66–73.

Guo, Z. G., Z. S. Yang, K. Lei, Y. Qu, and D. Fan. 1999. "Seasonal Variation of the Sedimentary Dynamic Processes for the Mud Area in the Northern East China Sea." *Journal of Ocean University of Qingdao* 3: 507–513.

Guo, Z. G., Z. S. Yang, D. Q. Zhang, D. J. Fan, and K. Lei. 2002. "Seasonal Distribution of Suspended Matter in the Northern East China Sea and Barrier Effect of Current Circulation on Its Transport." [In Chinese.] *Acta Oceanologica Sinica* 24 (5): 71–80.

Ichikawa, H., and R. C. Beardsley. 2002. "The Current System in the Yellow and East China Seas." *Journal of Oceanography* 58: 77–92. doi:10.1023/A:1015876701363.

IOCCG. 2000. "Remote Sensing of Ocean Color in Coastal, and Other Optically-Complex, Waters." In *Reports of the International Ocean-Color Coordinating Group, No. 3*, edited by S. Sathyendranath. Dartmouth: IOCCG.

Kessarkar, P. M., V. P. Rao, R. Shynu, I. M. Ahmad, P. Mehra, G. S. Michael, and D. Sundar. 2009. "Wind-Driven Estuarine Turbidity Maxima in Mandovi Estuary, Central West Coast of India." *Journal of Earth System Science* 118 (4): 369–377. doi:10.1007/s12040-009-0026-5.

Krivtsov, V., M. J. Howarth, and S. E. Jones. 2009. "Characterising Observed Patterns of Suspended Particulate Matter and Relationships with Oceanographic and Meteorological Variables: Studies

in Liverpool Bay." *Environmental Modelling & Software* 24: 677–685. doi:10.1016/j.envsoft.2008.09.012.
Li, J., Q. He, and H. Xu 2001. "The Fluid Mud Transportation Processes in Changjiang River Estuary."[In Chinese.] *Oceanologia Et Limnologia Sinica* 32 (3): 302–310.
Li, J., W. Shi, and H. Shen. 1994. "Sediment Properties and Transportation in the Turbidity Maximum in Changjiang Estuary." *Geographical Research* 13: 51–59.
Liu, J. P., K. H. Xu, A. C. Li, J. D. Milliman, D. M. Velozzi, S. B. Xiao, and Z. S. Yang. 2007. "Flux and Fate of Yangtze River Sediment Delivered to the East China Sea." *Geomorphology* 85: 208–224. doi:10.1016/j.geomorph.2006.03.023.
Lorenz, E. N. 1956. "Empirical Orthogonal Functions and Statistical Weather Prediction." *Scientific Report 1, Statistical Forecasting Project*, 49 pp (Defense Doc. Center No. 110268). Cambridge, MA: MIT. 49.
Milliman, J. D., and R. C. Meade. 1983. "World-Wide Delivery of River Sediment to the Oceans." *The Journal of Geology* 91: 1–21. doi:10.1086/628741.
Nezlin, N. P., and J. C. Mcwilliams. 2003. "Satellite Data, Empirical Orthogonal Functions, and the 1997–1998 El Niño off California." *Remote Sensing of Environment* 84 (2): 234–254. doi:10.1016/S0034-4257(02)00109-8.
Pang, C. G., F. Wang, X. Z. Bai, and M. H. Zhang. 2003. "Distribution Features of Suspended Matter and Amount of Sediment at the Changjiang Estuary and Adjacent Area." *Marine Sciences* 27: 31–35.
Powell, T. M., J. E. Cloern, and L. M. Huzzey. 1989. "Spatial and Temporal Variability in South San Francisco Bay (USA). I. Horizontal Distributions of Salinity, Suspended Sediments, and Phytoplankton Biomass and Productivity." *Estuarine, Coastal and Shelf Science* 28: 583–597. doi:10.1016/0272-7714(89)90048-6.
Schoellhamer, D. H. 1996. "Factors Affecting Suspended-Solids Concentrations in South San Francisco Bay, California." *Journal of Geophysical Research* 101 (C5): 2087–12095.
Shen, F., W. Verhoef, Y. X. Zhou, M. S. Salama, and X. L. Liu. 2010. "Satellite Estimates of Wide-Range Suspended Sediment Concentrations in Changjiang (Yangtze) Estuary Using MERIS Data." *Estuaries and Coasts* 33: 1420–1429. doi:10.1007/s12237-010-9313-2.
Shen, H. T., and D. Pan. 2001. *Turbidity Maximum in the Changjiang Estuary*, 28–29, 194. Beijing: China Ocean Press in Chinese.
Su, Y. S. 1989. "A Survey of Geographical Environment Circulation System in the Huanghai Sea and East China Sea." *Journal of Ocean University of Qiangdao* 19: 145–158.
Tang, D., I. H. Ni, F. E. Müller-Karger, and Z. J. Liu. 1998. "Analysis of Annual and Spatial Patterns of czcs-Derived Pigment Concentration on the Continental Shelf of China." *Continental Shelf Research* 18: 1493–1515. doi:10.1016/S0278-4343(98)00039-9.
Tang, D., I. H. Ni, F. E. Müller-Karger, and I. Oh. 2004. "Monthly Variation of Pigment Concentrations and Seasonal Winds in China's Marginal Seas." *Hydrobiologia* 511: 1–15. doi:10.1023/B:HYDR.0000014001.43554.6f.
Tew-Kai, E., and F. Marsac. 2009. "Patterns of Variability of Sea Surface Chlorophyll in the Mozambique Channel: A Quantitative Approach." *Journal of Marine Systems* 77: 77–88. doi:10.1016/j.jmarsys.2008.11.007.
Wang, W., and W. Jiang. 2008. "Study on the Seasonal Variation of the Suspended Sediment Distribution and Transportation in the East China Seas Based on SeaWiFS Data." *Journal of Ocean University of China* 7 (4): 385–392. doi:10.1007/s11802-008-0385-6.
Warner, J. C., D. H. Schoellhamer, C. A. Ruhl, and J. R. Burau. 2004. "Floodtide Pulses after Low Tides in Shallow Subembayments Adjacent to Deep Channels." *Estuarine, Coastal and Shelf Science* 60 (2): 213–228. doi:10.1016/j.ecss.2003.12.011.
Witt, G., and H. Siegel. 2000. "The Consequences of the Oder Flood in 1997 on the Distribution of Polycyclic Aromatic Hydrocarbons (PAHs) in the Oder River Estuary." *Marine Pollution Bulletin* 40 (12): 1124–1131. doi:10.1016/S0025-326X(00)00066-7.
Wu, J. X., H. T. Shen, and C. Y. Xiao. 2001. "Sediment Classification and Estimation of Suspended Sediment Fluxes in the Changjiang Estuary, China." *Water Resources Research* 37: 1969–1979. doi:10.1029/2000WR900352.
Xing, F., Y. Wang, J. Gao, and X. Zou. 2010. "Seasonal Distributions of the Concentrations of Suspended Sediment along Jiangsu Coastal Sea." [In Chinese.] *Oceanologia Et Limnologia Sinica* 41: 459–468.

Yan, Z., and D. L. Tang. 2009. "Changes in Suspended Sediments Associated with 2004 Indian Ocean Tsunami." *Advances in Space Research* 43: 89–95. doi:10.1016/j.asr.2008.03.002.

Zhang, J., Y. Wu, T. C. Jennerjahn, V. Ittekkot, and Q. He. 2007. "Distribution of Organic Matter in the Changjiang (Yangtze River) Estuary and Their Stable Carbon and Nitrogen Isotopic Ratios: Implications for Source Discrimination and Sedimentary Dynamics." *Marine Chemistry* 106: 111–126. doi:10.1016/j.marchem.2007.02.003.

Zhang, X. F., D. L. Tang, Z. Z. Li, and F. P. Zhang. 2009. "The Effects of Wind and Rainfall on Suspended Sediment Concentration Related to the 2004 Indian Ocean Tsunami." *Marine Pollution Bulletin* 58: 1367–1373. doi:10.1016/j.marpolbul.2009.04.023.